Available online at www.sciencedirect.com
ScienceDirect
Journal of Membrane Science 284 (2006) 128–136
journal of MEMBRANE SCIENCE
www.elsevier.com/locate/memsci

ZrO_2 and TiO_2 membranes for nanofiltration and pervaporation Part 1. Preparation and characterization of a corrosion-resistant ZrO_2 nanofiltration membrane with a MWCO < 300

Tim Van Gestel *, Henk Kruidhof, Dave H.A. Blank, Henny J.M. Bouwmeester

Inorganic Materials Science, Department of Science and Technology and MESA+ Institute for Nanotechnology, University of Twente, P.O. Box 217, 7500 AE Enschede, The Netherlands

Received 29 March 2006; received in revised form 11 July 2006; accepted 12 July 2006
Available online 16 July 2006

Abstract

This paper reports the sol–gel preparation and subsequent characterization of ceramic multilayer membranes, comprising a mesoporous γ-Al_2O_3 or ZrO_2 interlayer and a microporous ZrO_2 toplayer. The optimized membranes show a molecular weight cut-off (MWCO) of 200–300 in standard nanofiltration tests after firing the ZrO_2 toplayer at 400 °C. For the all-ZrO_2 membrane, a detailed study was made of its corrosion behaviour. PEG-retention, MWCO and permeability were studied in dynamic corrosion tests using aqueous solutions both at low and high pH values. Long-term corrosion tests (4 weeks) at successive pH values of 2, 13 and 1 demonstrated no significant loss in performance for the membranes showing a MWCO in the range 200–300.

Keywords: Ceramic membrane; ZrO_2; Nanofiltration; PEG-retention; Corrosion behaviour

1. Introduction

Nanofiltration (NF) membranes are generally classified into two major groups: organic polymeric and inorganic ceramic membranes. Polymeric membranes constitute the most important group and have been commercially available for many years. They are relatively easy to prepare and can be produced cheaply at large scale. However, their application is limited to moderate temperatures and to feed streams which are not too corrosive. Much research has been done towards optimization of flux and selectivity, but also towards improving solvent stability and corrosion resistance of the polymeric membranes. To date, however, there are still many restrictions to the feed mixtures that can be handled. Ceramic membranes generally do possess a high thermal, chemical and mechanical stability. Nonetheless, they are less frequently considered for NF applications, because their fabrication is often more complex and, hence, more costly.

Main advantages of ceramic membranes include: (1) resistance against dissolution and swelling upon exposure to organic solvents; (2) ability to withstand high temperatures; (3) ability of exposure towards extreme pH values; (4) long service-life [1,2]. Materials considered for mesoporous and microporous membrane formation include γ-Al_2O_3, TiO_2, ZrO_2, SiO_2. Of these, γ-Al_2O_3 and SiO_2 are suitable for application in organic liquids, but these materials do not display high enough chemical stability at high and low pH values [3]. In these cases membranes made of TiO_2 and ZrO_2 are more likely to be preferred.

Much research has been focused towards development of ceramic membranes with a ZrO_2 or TiO_2 NF toplayer. Guizard et al. [4] prepared ZrO_2 membranes, using a zirconium salt as precursor. The authors reported retention of 85% for yellow acid ($M = 759$ g/mol). Etienne et al. [5] used a tubular support with a 5 nm γ-Al_2O_3 ultrafiltration layer and reported retention of 90% for a dextrane with $M = 10\,000$ g/mol in MWCO measurements. Julbe et al. [6,7] prepared two types of ZrO_2 membranes, using either a zirconium salt or a zirconium alkoxide as precursor. The first preparation route is similar to that described by Guizard et al. [4]. The second type of membrane was prepared following a polymeric sol–gel route, involving the preparation of nanometer-sized particles through use of a zirconium alkoxide precursor modified by acetylacetone. Vacassy

* Corresponding author. Tel.: +31 53 4892998; fax: +31 53 4894683.
E-mail address: t.van.gestel@fz-juelich.de (T. Van Gestel).

0376-7388/$ – see front matter © 2006 Elsevier B.V. All rights reserved.
doi:10.1016/j.memsci.2006.07.020

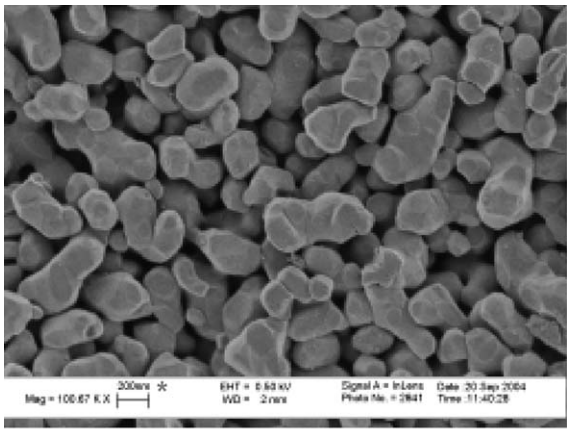

Fig. 1. FESEM micrograph of the surface (100 000×) of a macroporous AKP-30 membrane support.

et al. [8] used a polymeric sol–gel method to develop a ZrO_2 membrane on a commercial multichannel support with a ZrO_2 ultrafiltration layer (MWCO support = 15 000 Da). For the ZrO_2 toplayer, comprising 13 mol% of MgO, the following membrane performance was measured: saccharose (M = 342 g/mol) retention of 54% and Vitamin B_{12} (M = 1355 g/mol) retention of 73%. Benfer et al. [9] used a polymeric sol–gel method using either acetylacetone, diethanolamine or acetic acid as the modifier. For a tubular ZrO_2 membrane, an orange G (M = 452 g/mol) retention of 30% and a direct red (M = 991 g/mol) retention of 99% was measured.

Substantial progress has also been made towards development of NF membranes comprising a functional TiO_2 toplayer. Puhlfürß et al. [10] reported the preparation of TiO_2 NF membranes with a MWCO lower than 500, by a polymeric sol–gel method. The membranes were prepared on a support having a thin TiO_2 ultrafiltration layer (thickness 250 nm; pore size 5 nm). To date, similar membranes are offered commercially in a multichannel type configuration [11]. Benfer et al. [9] reported a polymeric sol–gel method using either acetylacetone, diethanolamine and acetic acid. For a tubular TiO_2 membrane, an orange G (M = 452 g/mol) retention of 45% and a direct red (M = 991 g/mol) retention of 97% was measured. Van Gestel et al. [12,13] prepared a TiO_2 disc membrane with a MWCO < 200 and a tubular membrane with a MWCO in the range 500–600. The difference in the performance was attributed to differences in the apparent surface roughness of the support and quality of the mesoporous TiO_2 interlayer. More recently, Sekulic [14] and Sekulic et al. [15] prepared a disc-shaped TiO_2 membrane on a γ-Al_2O_3 membrane interlayer, showing a triethylene glycol (M = 150 g/mol) retention of 65%, a PEG (M = 200 g/mol) retention of 75–80% and a PEG (M = 400 g/mol) retention of 90–95%. Tsuru et al. [16,17] reported fabrication of a TiO_2 membrane on a tubular α-Al_2O_3 support, with a diethylene glycol (M = 108 g/mol) retention of 40–50%, a sugar (M = 180 g/mol) retention of 75–80% and a raffinose (M = 504 g/mol) retention of >95%, and specify a MWCO of 250 for such a membrane. Voigt et al. [18] prepared TiO_2 membranes in a hollow fiber configuration showing a MWCO of about 250.

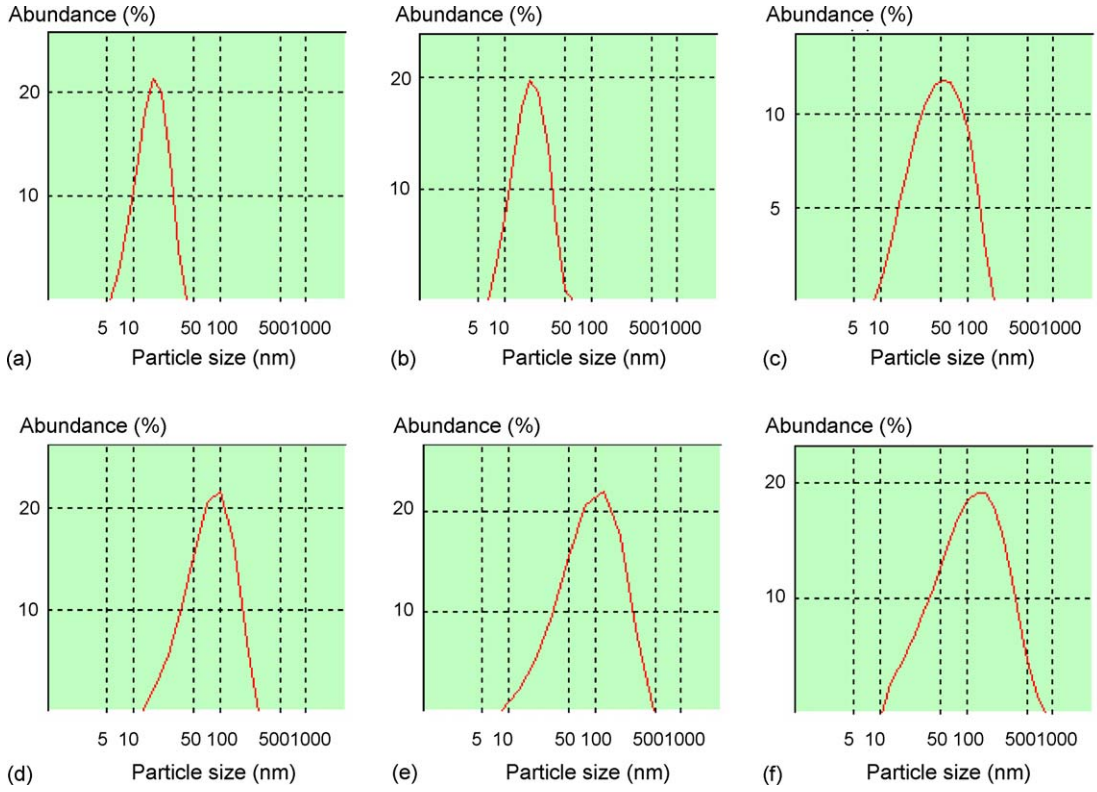

Fig. 2. Particle size distributions of colloidal zirconia sols with an average size: (a) <20 nm, (b) <30 nm, (c) 50 nm, (d) 100 nm, (e) 120 nm, and (f) 150 nm.

The goal of the present study was two-fold. First, to prepare a chemically stable microporous ZrO_2 membrane toplayer showing an improved performance in nanofiltration than the ZrO_2 membranes described (i.e. comparable with the TiO_2 membranes). Second, to measure the corrosion resistance of prepared membranes at low and high pH values. The development of microporous ZrO_2 and TiO_2 membranes with pore sizes smaller than those of the membranes described in the present study, together with results from standard pervaporation tests, will be discussed in a forthcoming paper (part II).

2. Experimental

2.1. Membrane preparation

2.1.1. Support

Membrane supports were prepared by vacuum slip-casting, starting from a commercially available α-Al_2O_3 powder (AKP-30, Sumitomo). A suspension of AKP-30 was made, treated ultrasonically and filtered through a 200 μm filter. From this suspension, green support discs with a diameter of about 40 mm were formed. These were dried and subsequently fired in air at 1100 °C for 1 h. Finally, discs containing diamond particles were used for polishing (metal bounded N 10 μm, paraffin wax bounded R 30, 10 μm).

2.1.2. Interlayers

Alumina and zirconia colloidal particulate sols were prepared using commercially available alkoxide precursors, which were hydrolyzed by the addition of an excess of H_2O. The γ-alumina sol was prepared by hydrolysis of Al-tri-*sec*-butoxide ($Al(OC_4H_9)_3$, Aldrich) followed by peptization with HNO_3, according to a procedure described previously [19–21]. The zirconia sol was prepared by hydrolysis of Zr-tetra-*n*-propoxide ($Zr(OC_3H_7)_4$, Aldrich). Yttria-doped zirconia sols (3 mol% yttria) were prepared by adding the proper amount of $Y(NO_3)_3{\cdot}6H_2O$ to the zirconia sol.

Supported gel-layers were formed on the membrane support by dip-coating. Before applying the layer, PVA was added as a drying chemical controlling additive (DCCA) to the final γ-alumina, zirconia or yttria-doped zirconia sols. Dip-coating was performed in a clean room, using an automatic dip-coating device (Velterop DA 3960/02). Unsupported gel-layers were obtained in a Petri dish from the remaining liquid.

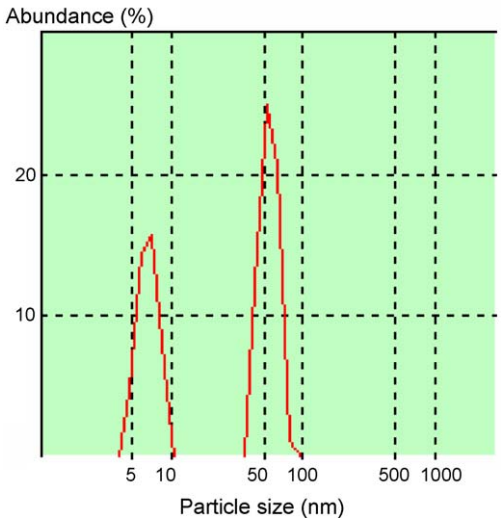

Fig. 3. Particle size distribution of a polymeric zirconia sol.

The obtained supported and unsupported gel-layers were dried at 40 °C at relative humidity of 60% in a climate chamber. In order to obtain the γ-Al_2O_3 membrane interlayer, firing was performed in air at 600 °C for 3 h. In the case of ZrO_2 and Y_2O_3-doped ZrO_2 interlayers, firing took place at 400 or 450 °C. Unless stated otherwise, the entire dip-coating – drying – firing cycle was carried out once for forming a γ-Al_2O_3 interlayer and twice for a ZrO_2 interlayer.

2.1.3. Toplayers

A polymeric zirconia sol was produced using Zr-tetra-*n*-propoxide ($Zr(OC_3H_7)_4$, Aldrich), which was partially hydrolyzed with a less than equivalent amount of H_2O. In order to obtain a precipitate-free zirconia sol, the reactivity of the precursor was reduced prior to hydrolysis, by addition of acetylacetone. This was done under He in a glove box. The obtained sol appeared stable and suitable for dip-coating. Subsequently, a gel-layer was applied onto the support and converted into the final ZrO_2 toplayer by subsequent drying and firing in air for 2 h. No drying controlling agents or other additives were used.

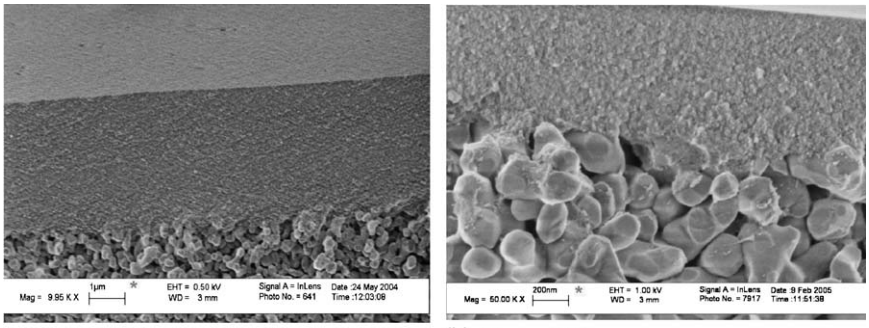

Fig. 4. FESEM micrographs of the cross-section of (a) γ-Al_2O_3 and (b) 3% Y_2O_3-doped ZrO_2 colloidal sol–gel derived membrane layers on an α-Al_2O_3 support ((a) 10 000× and (b) 50 000×).

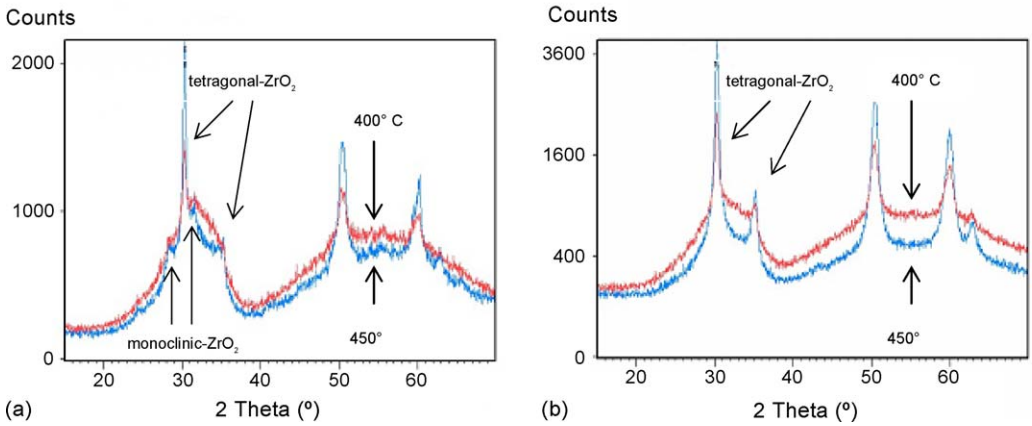

Fig. 5. XRD patterns of (a) ZrO_2 and (b) 3 mol% Y_2O_3-doped ZrO_2 colloidal sol–gel derived materials fired at 400 and 450 °C.

Unless stated otherwise, a firing temperature of 400 °C was used and the dip-coating – drying – firing cycle was carried out twice.

2.2. Characterization

2.2.1. Structural characterization

The membrane support was characterized by field emission-scanning electron microscopy (FESEM, LEO Gemini 1550), X-ray diffraction and Hg-porosimetry. The particle size of the colloidal and polymeric sols was determined by laser scattering (ZetaSizer 3000Hsa, Malvern). Membrane interlayers and toplayers were characterized by FESEM, optical microscopy, X-ray diffraction and N_2-adsorption/desorption pore measurements (Micromeritics, ASAP 2400). The last two methods were carried out on unsupported membrane layers, assuming that the structural properties are similar to those of supported membrane layers.

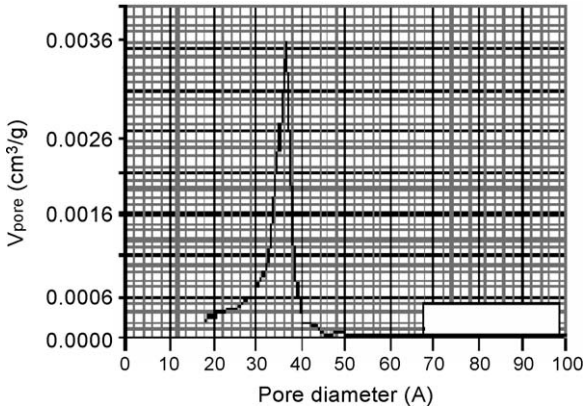

Fig. 6. Pore size distribution of 3 mol% Y_2O_3-doped ZrO_2 colloidal sol–gel derived material fired at 450 °C.

2.2.2. Filtration tests

Membranes were tested in a set-up for liquids, consisting of a stainless-steel permeation vessel being connected to a He gas cylinder. During the permeation/filtration tests, the temperature inside the vessel was kept at 25 °C. A feed volume of 2.5 l was taken and the liquid was continuously stirred in order to avoid the occurrence of concentration gradients. For analysis of retention, standard ultrafiltration (UF) and nanofiltration (NF) tests with aqueous polyethylene glycol solutions (PEG, Merck) were performed. For the UF test, the feed solution contained PEGs with molecular masses of 600, 1500, 3000 and 10 000. For the NF test, the feed solution contained PEGs with molecular masses of 200, 600 and 1500. The overall PEG concentration in both tests was 3 g/l. During each test, samples of the feed and permeate solutions were collected at a pressure of 10 bar. Analysis of the composition of these samples was conducted by gel permeation chromatography (GPC, Waters). The molecular mass of the PEG corresponding to a 90% retention level was taken as the MWCO of the membrane.

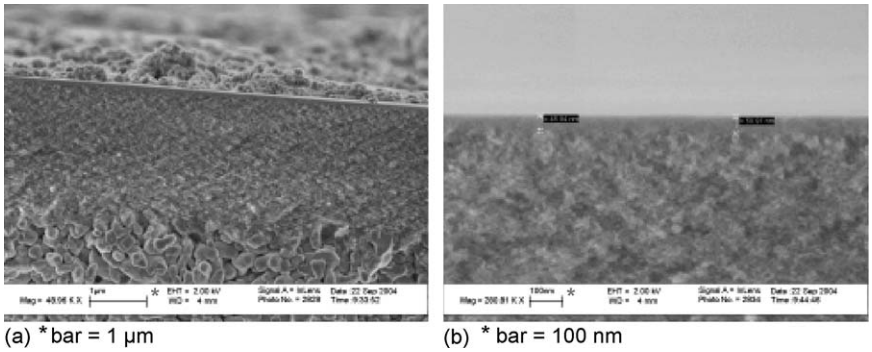

Fig. 7. FESEM micrographs of the cross-section of a multilayer α-Al_2O_3/γ-Al_2O_3/ZrO_2 membrane ((a) 50 000× and (b) 280 000×; toplayer fired at 400 °C).

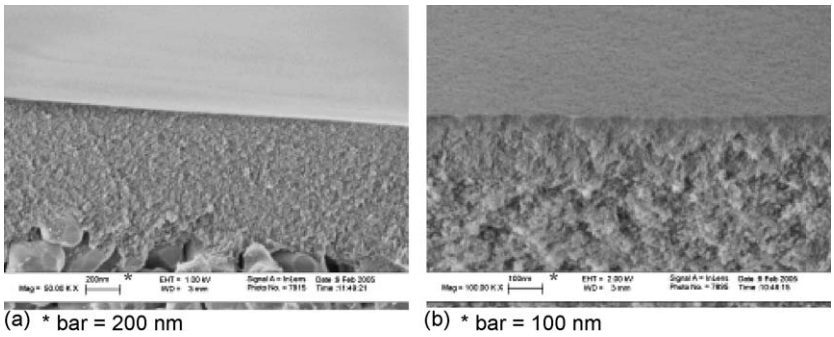

Fig. 8. FESEM micrographs of the cross-section of a multilayer α-Al_2O_3/ZrO_2/ZrO_2 membrane ((a) 50 000× and (b) 100 000×; toplayer fired at 400 °C).

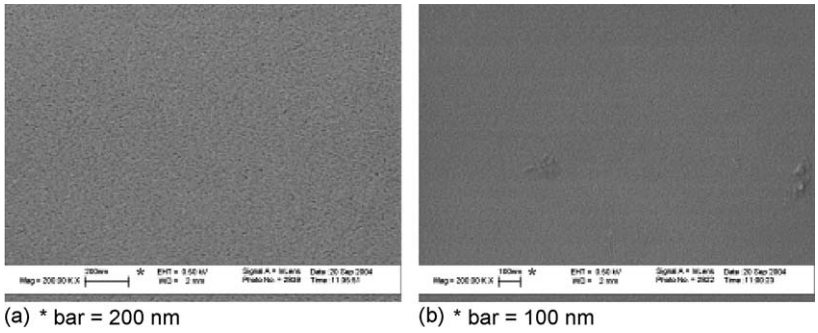

Fig. 9. FESEM micrographs of the membrane surface (a) before and (b) after the polymeric sol–gel dip-coating procedure ((a) 200 000× and (b) 200 000×; toplayer fired at 400 °C).

2.2.3. *Corrosion tests*

The membrane was enclosed in the permeation vessel, as described in the previous section. The procedure of the corrosion test was as follows: (1) first membrane performance characterization (PEG-retention, MWCO); (2) permeation of the corrosive feed solution for 2 weeks; (3) second membrane performance characterization; (4) applying a fresh feed solution. As feed, solutions of HNO_3 and NaOH were used in the order: pH = 2 (2 × 2 weeks), pH = 13 (2 × 2 weeks) and pH = 1 (2 × 2 weeks). During the entire test period, which lasted about 3 months, the membrane was kept inside the vessel, unless membrane degradation was observed. After 1 month of testing at pH 2, the feed solution was changed for the solution with pH 13. After another month of testing, the feed solution was changed for the solution with pH 1. All testing was carried out at a transmembrane pressure in the range 5–7 bar at a temperature of 25 °C.

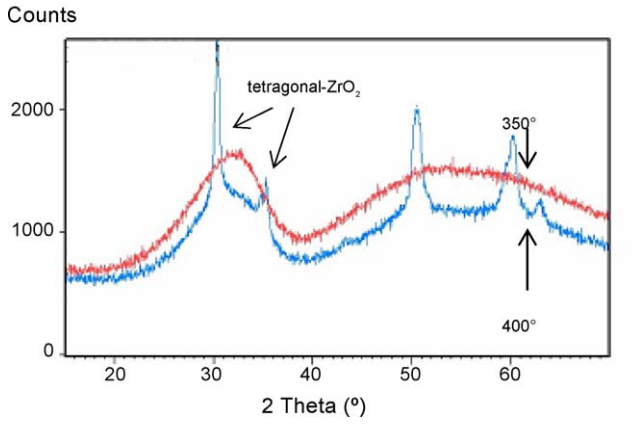

Fig. 10. XRD patterns of polymeric sol–gel derived ZrO_2 material fired at 350 and 400 °C.

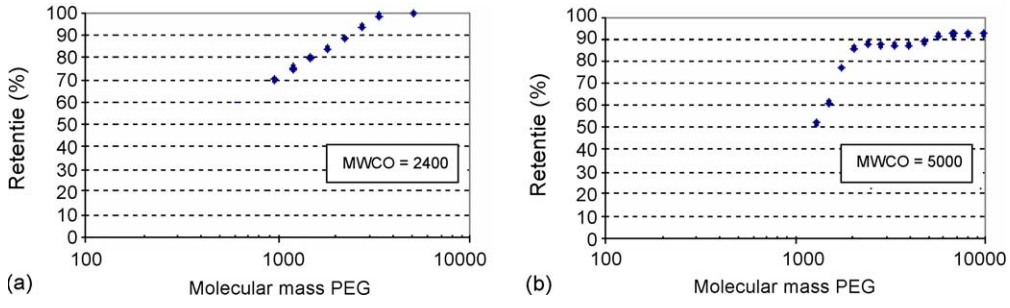

Fig. 11. PEG retention curves for (a) γ-Al_2O_3 and (b) 3 mol% Y_2O_3-doped ZrO_2 interlayers.

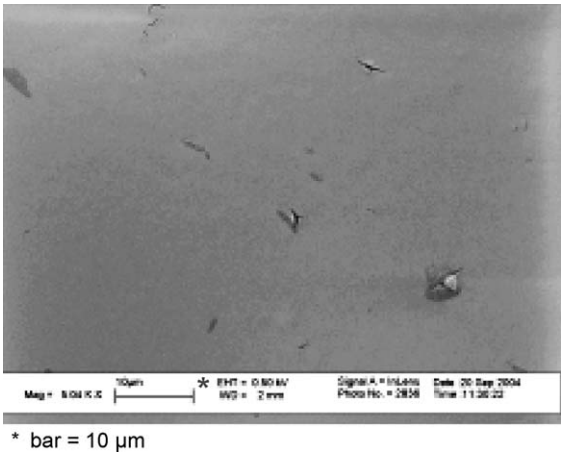

Fig. 12. FESEM micrograph of the surface of a 3 mol% Y_2O_3-doped ZrO_2 interlayer (5000×).

3. Results and discussion

3.1. Membrane preparation

3.1.1. Support

The FESEM micrograph (Fig. 1) of the membrane support shows that our method results in a typical macroporous structure. Optical microscopy and visual inspection confirmed that the polishing procedure leads to a very smooth surface. Structural characterization indicated an α-Al_2O_3 phase, an estimated pore size of ∼80 nm and a porosity of 35–40% after firing at 1100 °C. Long-term corrosion tests in HNO_3 solutions conducted on a similar α-Al_2O_3 membrane support confirmed a high chemical stability for this support material [12]. For example, only very small amounts of dissolved aluminium (571 μg/l) were found after an exposure of 6 months at pH 1.

3.1.2. Sols

For the formation of mesoporous membrane interlayers, sols with relatively large nanometer-sized particles were aimed at. This was obtained by reacting the alkoxide precursors with a large excess of H_2O. The final products after peptization were stable colloidal γ-alumina and zirconia sols. A state-of-the-art γ-alumina sol, containing particles with an average diameter in the range 60–100 nm, was used for the formation of the mesoporous γ-Al_2O_3 interlayer. For the development of the mesoporous ZrO_2 interlayer, a series of stable zirconia sols was prepared, having different particle sizes. The average particle size varied between 15 and 150 nm. Particle size distributions of 6 representative sols are shown in Fig. 2. Sols having the smallest zirconia particles (sol a–c) were not suitable for dip-coating, due to excessive penetration of particles into the pores of the support. Stable sols having zirconia particles with an average size of ∼100 nm were therefore used for membrane preparation. The visual appearance of the latter zirconia sol and the γ-alumina sol was similar. Both were semi-transparent with a light blue appearance, indicating the presence of relatively large particles. For formation of the microporous ZrO_2 toplayer, a precipitate-free polymeric sol was prepared. Fig. 3 shows that the particle size distribution of the sol is bimodal, comprising two types of polymeric structures: structures with a size in the range 5–10 nm and larger ones with an estimated size of ∼50 nm. In contrast with the colloidal sols, the polymeric sol was completely transparent.

3.1.3. Membrane interlayers

3.1.3.1. Morphology. Fig. 4 shows FESEM micrographs of γ-Al_2O_3 and 3 mol% Y_2O_3-doped ZrO_2 interlayers, prepared according to the colloidal sol–gel dip-coating procedure. From these images it is apparent that the thickness of the membrane interlayers is strongly dependent on the type of material used. Using γ-Al_2O_3, an interlayer of thickness 2 μm or more could easily be obtained by dip-coating twice. Therefore, applying two layers is not strictly required for this membrane material, but in practice can be used for surface smoothening. The preparation of a crack-free ZrO_2 or Y_2O_3–ZrO_2 interlayer with sufficient thickness appeared to be more difficult. Only very thin crack-free layers could be obtained, so that a second dip-coating was necessary to increase membrane thickness and to reduce surface roughness of the support. ZrO_2 and Y_2O_3–ZrO_2 interlayers obtained in this way showed an average thickness of ca. 0.3–0.4 μm.

3.1.3.2. Structural properties. The γ-Al_2O_3 interlayer was prepared according to the method described in Refs. [19–21]. After firing at 600 °C, a typical average pore size of 3–4 nm was measured (BJH model). For the ZrO_2 and 3 mol% Y_2O_3–ZrO_2 membrane interlayers, the firing was either at 450 or 400 °C. A lower firing temperature was not considered, because of the risk of insufficient burning out the drying controlling additive (PVA).

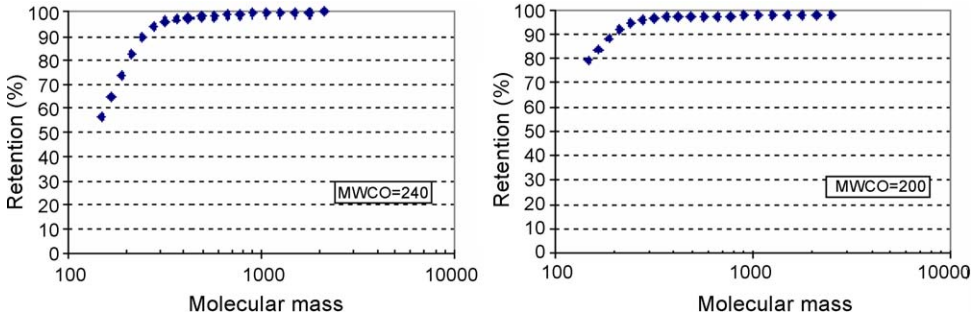

Fig. 13. PEG-retention curves for (a) α-Al_2O_3/γ-Al_2O_3/ZrO_2 and (b) α-Al_2O_3/ZrO_2/ZrO_2 multilayer membranes.

After firing at 400 °C, the tetragonal polymorph of zirconia was found for both membrane materials (Fig. 5). Pore analysis indicated a mesoporous structure (type IV isotherm) and an average pore size of 3–4 nm, which is similar to that found for γ-Al_2O_3. After firing at 450 °C, the XRD pattern of the pure ZrO_2 interlayer material shows peaks of the tetragonal phase along with some small peaks of the monoclinic phase (Fig. 5a). The tetragonal-monoclinic phase transformation is undesired since it may induce stress in the membrane layer and enhances the risk of crack-formation. For the 3 mol% Y_2O_3–ZrO_2 membrane material, on the other hand, XRD confirmed single phase behaviour (Fig. 5b). Since a firing temperature of 450 °C is also more preferred to remove PVA, 3 mol% Y_2O_3–ZrO_2 was selected for formation of the interlayer in the multilayer structure. In Fig. 6, the pore size distribution measured for this membrane material is shown.

3.1.4. Membrane toplayer

3.1.4.1. Morphology. Fig. 7 shows FESEM micrographs of a ZrO_2 toplayer, coated on a mesoporous γ-Al_2O_3 interlayer after firing at 400 °C. In Fig. 7a, a typical multilayer structure can be observed comprising the macroporous α-Al_2O_3 support, mesoporous interlayer and microporous toplayer. It appears that a uniform and separate toplayer has been formed and that penetration of the sol particles into the interlayer pores did not occur. The irregularities on the upper side of the toplayer are dust particles, which accumulated on the surface during filtration tests with polluted colour containing feed streams. Fig. 7b shows the same toplayer at a higher magnification. From this micrograph, an average membrane thickness of ∼50 nm was estimated.

Fig. 8 shows a cross-sectional FESEM micrograph taken after coating a ZrO_2 toplayer on a mesoporous ZrO_2 interlayer. In contrast with the previous micrographs, a separate toplayer cannot so easily be observed, due to the similarity of the membrane interlayer and toplayer material. Therefore, surface micrographs made before and after the toplayer coating procedure are also provided (Fig. 9). Fig. 9a shows the membrane surface before performing the polymeric sol–gel dip-coating procedure, which implies that this corresponds to the surface of the mesoporous ZrO_2 membrane interlayer. Fig. 9b shows the surface after dip-coating and firing. By comparing these pictures, it appears that a layer with a finer pore structure is formed on the membrane interlayer. It is, however, not clear to which extent the toplayer material has penetrated into the pores of the interlayer or that a separate toplayer has been formed.

3.1.4.2. Structural properties. Fig. 10 shows the XRD patterns of the ZrO_2 toplayer material after firing at 350 and 400 °C. At the lowest temperature, the phase is mainly amorphous. At 400 °C, formation of the tetragonal structure is observed.

3.2. Filtration tests

3.2.1. Membrane interlayer

Fig. 11 shows PEG retention curves measured for γ-Al_2O_3 and 3 mol% Y_2O_3–ZrO_2 membrane interlayers. Based on these retention data, both layers can be characterized as tight UF membranes, having a pore size in the lower mesoporous range [10]. The γ-Al_2O_3 interlayer shows the properties of a very tight UF membrane with a MWCO of ∼2500. For the Y_2O_3–ZrO_2 interlayer, the MWCO is somewhat higher (∼5000) and the retention curve does not reach 100%. Since the pore sizes measured for both membrane materials using gas adsorption/desorption are largely comparable, this difference in retention behaviour is attributed to the presence of small defects in the relatively thin Y_2O_3–ZrO_2 interlayer as confirmed by SEM analysis (Fig. 12). Defects could not be revealed by SEM analysis of the γ-Al_2O_3 interlayer.

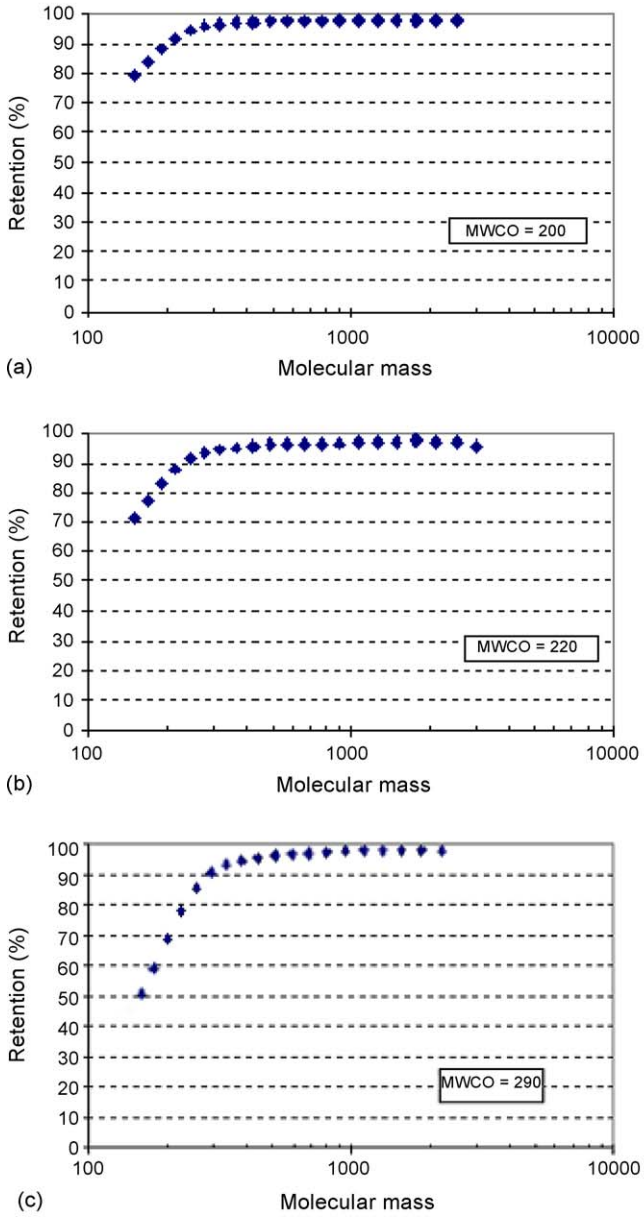

Fig. 14. PEG-retention curves for the corrosion test with a HNO_3 solution at pH 2 obtained (a) before permeation, (b) after 2 weeks of permeation, and (c) after 4 weeks of permeation.

3.2.2. Membrane toplayer

Fig. 13 shows PEG retention data measured for the ZrO_2 membrane toplayer coated on either γ-Al_2O_3 or ZrO_2 membrane interlayers. The measured permeabilities are 2.56 and 2.28 $l\,h^{-1}\,m^{-2}\,bar^{-1}$, respectively. It is apparent that similar retention behaviour is obtained for both membranes. A high retention was found for the smallest PEG molecules and, therefore, the membrane toplayer in either case can be characterized as a tight NF membrane (MWCO < 300). In practice, formation of a ZrO_2 toplayer with a MWCO lower than 300 on top of a smooth high-quality γ-Al_2O_3 interlayer appeared easily. Unfortunately, γ-Al_2O_3 interlayers are only chemically stable in non-aqueous or mild aqueous liquids (pH 3–10). They also cannot be considered for application in strong acid or alkaline media [12,22]. Coating of the ZrO_2 microporous toplayer on the mesoporous ZrO_2 interlayer was experienced to be much more difficult, which was attributed to the lower quality of the ZrO_2 interlayers in this study. However, for said reasons of stability (see Section 1), main interest in this study was in testing of a NF membrane consisting of a ZrO_2 toplayer with a MWCO < 300 coated on a ZrO_2 interlayer.

3.3. Corrosion tests

Fig. 14 shows PEG retention data of the ZrO_2 toplayer supported on a ZrO_2 interlayer measured before (a), after 2 weeks (b) and 4 weeks (c) of permeation with a solution with a pH 2.

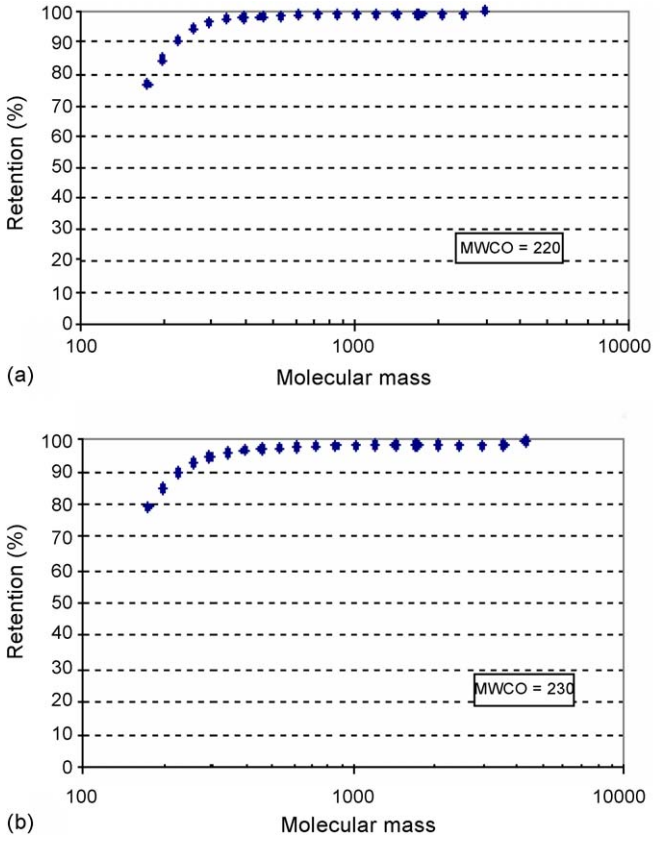

Fig. 15. PEG-retention curves for the corrosion test with a NaOH solution at pH 13 obtained (a) after 2 weeks of permeation and (b) after 4 weeks of permeation.

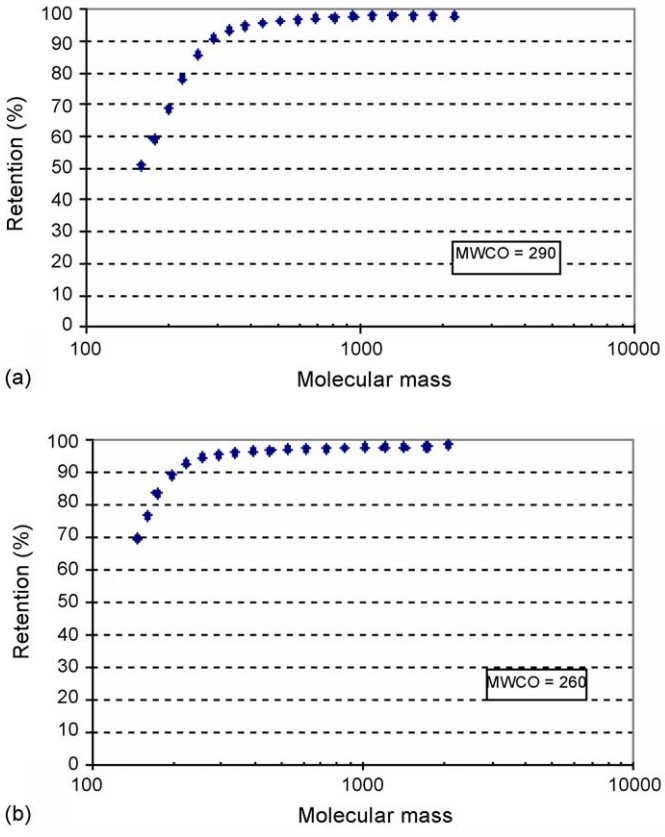

Fig. 16. PEG–retention curves for the corrosion test with a HNO_3 solution at pH 1 obtained (a) after 2 weeks of permeation and (b) after 4 weeks of permeation.

Figs. 15 and 16 show data of subsequent tests at pH 13 and 1, respectively. Besides some small changes in PEG-retention and MWCO, no significant membrane corrosion has taken place. The permeability measured during the last PEG retention test (after the last corrosion test) was 2.35 $l\,h^{-1}\,m^{-2}\,bar^{-1}$, which is a similar value as at the start of the corrosion tests.

4. Conclusions

In this study, ceramic membranes with excellent NF properties were obtained using a sol–gel dip-coating procedure. The ZrO_2 toplayer of thickness ~50 nm was identified as the tetragonal polymorph of ZrO_2. Either mesoporous γ-Al_2O_3 or tetragonal ZrO_2 were used as interlayers. In standard PEG-retention tests, both type of membranes showed a MWCO in the range 200–300. The ZrO_2 toplayer coated on a ZrO_2 interlayer demonstrated high stability in a series of corrosion tests with feed solutions having a pH value of 2, 13 and 1. From this, it is suggested that the ZrO_2 ceramic membrane could have a widespread application in NF for either acid or alkaline feed streams.

Acknowledgements

This work was supported with a grant of the Dutch Programme EET (Economy, Ecology, Technology). Frans Servaes, Jean-Pierre Moreels and Anita Buekenhoudt (Vito, Belgium) are

gratefully acknowledged for providing the GPC results. Mark Smithers (Central Materials Analysis Laboratory, University of Twente) is gratefully thanked for SEM measurements.

References

[1] A.J. Burggraaf, L. Cot, Fundamentals of Inorganic Membrane Science and Technology, in: Elsevier Science and Technology Series No. 4, Elsevier, Amsterdam, 1996.
[2] R.R. Bhave, Inorganic Membranes: Characterization and Applications, van Nostrand Reinhold, New York, 1991.
[3] J.M. Hofman-Züter, Chemical and thermal stability of mesoporous ceramic membranes, PhD Thesis, University of Twente, Enschede, The Netherlands, 1995.
[4] C. Guizard, A. Julbe, A. Larbot, L. Cot, Nanostructures in sol–gel derived materials. Application to the elaboration of nanofiltration membranes, Key Eng. Mater. 61/62 (1991) 47–56.
[5] J. Etienne, A. Larbot, A. Julbe, L. Cot, A microporous zirconia membrane prepared by the sol–gel process from zirconyl oxalate, J. Membr. Sci. 86 (1994) 95.
[6] A. Julbe, C. Guizard, A. Larbot, L. Cot, A. Giroir-Fendler, The sol–gel approach to prepare candidate microporous inorganic membranes for membrane reactors, J. Membr. Sci. 77 (1993) 137–153.
[7] A. Julbe, C. Guizard, A. Larbot, C. Mouchet, R. Vacassy, R. Metz, L. Cot, Sol–gel processing of zirconia and titania membranes, MRS Symposium Proceedings No. 273.
[8] R. Vacassy, C. Guizard, V. Thoraval, L. Cot, Synthesis and characterisation of microporous zirconia powders. Application in nanofiltration characteristics, J. Membr. Sci. 132 (1997) 109–118.
[9] S. Benfer, U. Popp, H. Richter, C. Siewert, G. Tomandl, Development and characterization of ceramic nanofiltration membranes, Sep. Purif. Technol. 22/23 (2001) 231–237.
[10] P. Puhlfürß, A. Voigt, R. Weber, M. Morbé, Microporous TiO_2 membranes with a cut-off <500 Da, J. Membr. Sci. 174 (2000) 123–133.
[11] http://www.inopor.com/en/membranes_e.html.
[12] T. Van Gestel, C. Vandecasteele, A. Buekenhoudt, C. Dotremont, J. Luyten, R. Leysen, B. Van der Bruggen, G. Maes, Alumina and titania multilayer membranes for nanofiltration: preparation, characterization and chemical stability, J. Membr. Sci. 207 (2002) 73–89.
[13] T. Van Gestel, C. Vandecasteele, A. Buekenhoudt, C. Dotremont, J. Luyten, R. Leysen, B. Van der Bruggen, G. Maes, Salt retention in nanofiltration with multilayer ceramic TiO_2 membranes, J. Membr. Sci. 209 (2002) 379–389.
[14] J. Sekulic, Mesoporous and microporous titania membranes, PhD Thesis, University of Twente, Enschede, The Netherlands, 2004.
[15] J. Sekulic, J.E. ten Elshof, D.H.A. Blank, A microporous titania membrane for nanofiltration and pervaporation, Adv. Mater. 72 (2004) 49–57.
[16] T. Tsuru, D. Hironka, T. Yoshioka, M. Asaeda, Titania membranes for liquid phase separation: effect of surface charge on flux, Sep. Purif. Technol. 25 (2001) 307–314.
[17] T. Tsuru, D. Hironka, T. Yoshioka, M. Asaeda, Effect of divalent cations on permeate volume flux through porous titania membranes, Desalination 147 (2002) 213–216.
[18] I. Voigt, G. Fisher, P. Puhlfürß, M. Schleifenheimer, M. Stahn, TiO_2 NF-membranes on capillary supports, Sep. Purif. Technol. 32 (2003) 87–91.
[19] A.J. Burggraaf, K. Keizer, Synthesis of Inorganic membranes, in: R.R. Bhave (Ed.), Inorganic Membranes: Characterization and Applications, van Nostrand Rheinhold, New York, 1991, pp. 10–63.
[20] V.T. Zaspalis, W. Van Praag, K. Keizer, J.R.H. Ross, A.J. Burggraaf, Synthesis and characterization of primary alumina, titania and binary membranes, J. Mater. Sci. 27 (1992) 1023–1035.
[21] K.N. Kumar, Nanostructured ceramic membranes: layer and texture formation, PhD Thesis, University of Twente, Enschede, The Netherlands, 1993.
[22] T. Van Gestel, C. Vandecasteele, A. Buekenhoudt, C. Dotremont, J. Luyten, R. Leysen, B. Van der Bruggen, G. Maes, Corrosion properties of alumina and titania NF membranes, J. Membr. Sci. 214 (2003) 21–29.